Proceedings of the Korean Nuclear Society Autumn Meeting, 2001

Estimation of Microstructures and Material Properties of HAZ in SA508 Reactor Pressure Vessel

J.S. Kim*, S.G. Lee, J.S. Park and T.E. Jin

Welding Integrity in Nuclear Structures Laboratory (www.wins.re.kr)
Korea Power Engineering Company
360-9, Mabuk-ri Kusong-eup Yongin-si, Kyunggi-do, Korea

ASTRACT

To perform the rigorous integrity evaluation of RPV, it is necessary to consider metallurgical factors such as microstructure evolution during multi-pass welding process and PWHT. The microstructures of the heat affected zone(HAZ) of SA508 steel were predicted by a combination of simulated thermal analysis and a simple kinetic models for austenite grain growth and austenite-ferrite transformation. Phase equilibrium of SA508 steel was calculated using a Thermo-Calc package. Carbide growth in the HAZ was predicted by a empirical model, taking into account the predicted microstructure evolution. Finally, these prediction results are compared with experimental ones and show the reasonable agreement.

1. INTRODUCTION

The metallurgical microstructures of HAZ are changed due to repeated thermal cycle during multi-pass welding and carbides coarsening during PWHT. Especially, in case of SA508 steel, which has been widely used for pressure vessel because of good mechanical properties, the mechanical properties of HAZ may be degraded due to the microstructure change. Therefore, the some studies(Ref. 1~4) has been performed for more detailed estimation of the microstructures and material properties for HAZ of SA508 steel. However, these studies used the experimental approaches, so it has the economic problems to apply the methodologies used in these studies to various welding processes and geometric shapes.

Accordingly, the purpose of this study is to estimate the microstructures and material properties for the HAZ of SA508 Gr.3 Cl.1, which has been often used for RPV. The microstructures of HAZ are predicted by a combination of the temperature analysis considering multi-pass welding

and PWHT, and the thermodynamics-kinetics models for prior-austenite grain growth, austenite decomposition and carbide coarsening. Also, the as-welded hardness, yielding strength and tensile strength are estimated by the prediction results for microstructures and the empirical relations.

2. METHODOLOGY

Fig. 1 shows a methodology for the microstructures and mechanical properties estimation of the HAZ in SA508 Gr.3 Cl.1. As shown in Fig. 1, firstly, thermal analysis is performed to determine the peak temperature and cooling rate in HAZ considering real welding processes such as multi-pass welding and PWHT. Secondly, the microstructures of HAZ are estimated considering various metallurgical factors such as prior-austenite grain growth and austenite decomposition during welding. In addition, the carbide coarsening during PWHT is also estimated. Finally, the changes of mechanical properties due to microstructure changes are predicted.

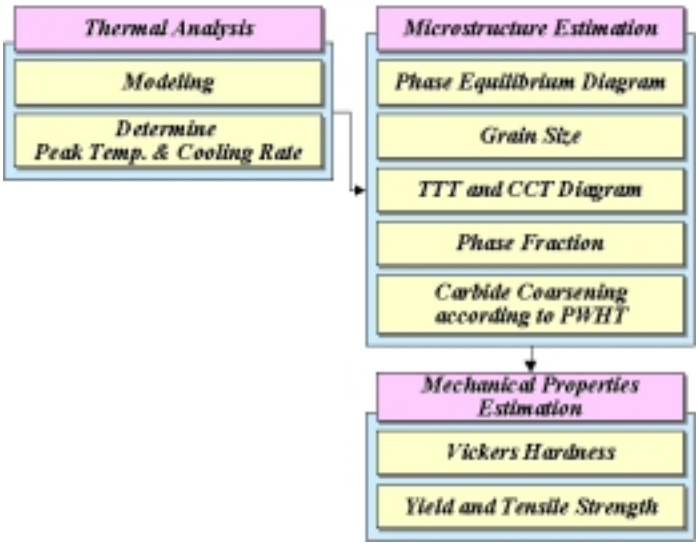

Fig. 1. Methodology of microstructure estimation.

3. TEMPERATURE ANALYSIS

Analysis Model

Fig. 2 shows the analysis model of RPV circumferential narrow gap weld. Base material is SA 508 Gr.3 Cl.1 and filler material is L-TEC 44. Submerged arc welding(SAW) method is used in the narrow gap weld. Welding is performed with 81 passes and 39 passes for inner and outer part respectively. Table 1 summarizes the chemical compositions of SA 508 Gr.3 Cl.1 for RPV. And Table 2 summarizes the welding parameters of this model.

Finite Element Model

The finite element for an analysis model is shown in Fig. 3. The numbers of elements and nodes are 830 and 940 respectively. The element property is a 4-node axis-symmetric element (Ref. 5). By using the lumped model(Ref. 6), the finite element model is simplified as the one with 8 and 5 weld layers for inner and outer weld part respectively. Model change technique(Ref. 5) is adopted to simulate multi-pass welding process.

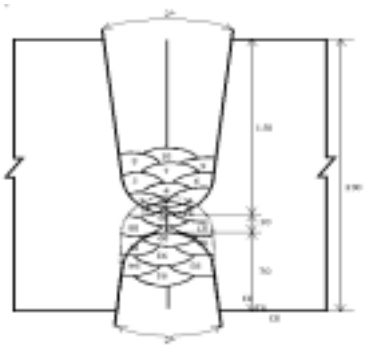

Fig. 2. Analysis model.

Table 1. Chemical composition of SA508 Gr.3 Cl.1

Element	C	Si	Mn	P	S	Ni	Cr	Mo
wt.%	0.19	0.08	1.35	0.006	0.002	0.82	0.17	0.51

Table 2. Specifications of welding parameters

Wire Size	Current	Voltage	Speed	Preheat temp.	Interpass temp.	PWHT
4mm	500～600A	28～32V	30～40 cm/min	121℃(min.)	200℃(max.)	615℃/ 40hr

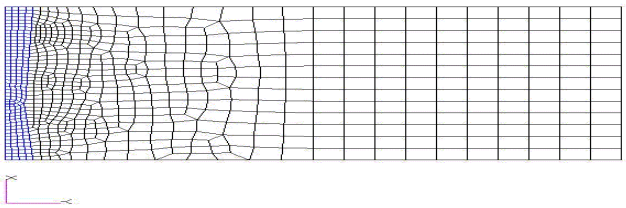

Fig. 3. Finite element model.

Analysis Results

As shown in Fig. 4, temperature cycle in HAZ is the saw-tooth pattern because of repeated heating and cooling during multi-pass welding.

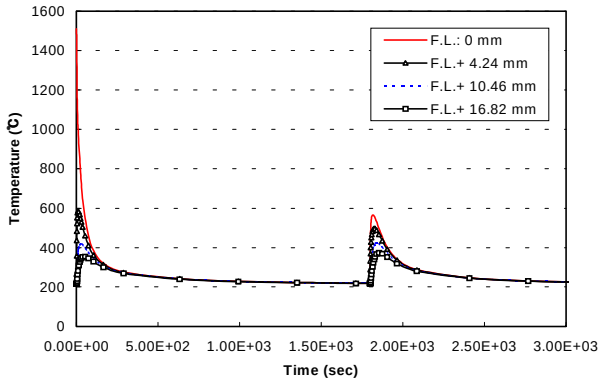

Fig. 4. Peak temperature change vs. time.

4. MICROSTRUCTURE PREDICTION

Determination of Equilibrium Phase Diagram

Fig. 5 shows the equilibrium phase diagram of SA508 Gr.3 Cl.1 according to temperature calculated by Thermo-Calc(Ref. 7). As shown in Fig. 5, the thermodynamically stable carbides are MC, M_2C, M_7C_3, ξ-carbide and cementite(M_3C). But, it is difficult that the MC type carbide precipitates because of relatively low temperature. These results show the good agreement with TEM analysis results that the carbides of M_2C and M_3C type are observed. Table 3 presents the equilibrium phase transformation temperatures from ferrite to austenite, A_{e1} and A_{e3}, determined from Fig. 5. From Table 3, these calculation results have a few differences in quantities from the previous results that are phase transformation temperatures during heating.

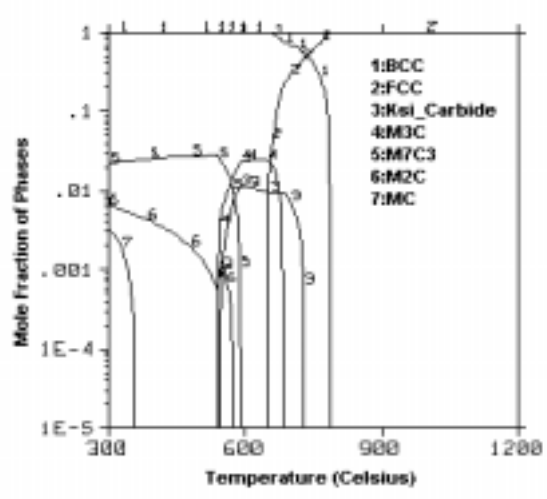

Fig. 5. Equilibrium mole fractions of phases vs. temperature for the SA508 Gr.3 Cl.1.

Table 3. Phase transformation temperatures from ferrite to austenite.

Tool \ Temperature	A_1(℃)	A_3(℃)	Remark
Thermo-Calc	646	790	A_{e1}/A_{e3}
Experiment (Ref. 8)	680	830	A_{c1}/A_{c3}
Experiment (Ref. 9)	701	786	A_{c1}/A_{c3}

Estimation of Grain Size

Grain size is an important factor to predict the microstructure because grain boundaries provide nucleation sites and diffusion paths. Therefore, the grain sizes of HAZ have to be estimated according to distance from fusion line before determination of TTT(Time Temperature Transformation) and CCT(Continuous Cooling Transformation) diagrams. The grain sizes are predicted by using the following Svensson's equations(Ref. 10):

$$d_r^{1/n_1} = d_{r0}^{1/n_1} + K_0 \alpha \tau e^{-Q/RT_p} \quad (1)$$

$$\alpha = 2\sqrt{(\pi R T_p / Q)} \quad (2)$$

$$\tau = (q'/vd)/[2\pi\lambda\rho e(T_p - T_0)^2 \quad (3)$$

where, d_r is the time-dependent grain size, d_{r0} is the initial grain size, n_1 is an exponent, Q is the activation energy, T_p is the peak temperature, λ is thermal conductivity, and ρ is density. As shown in Fig. 6, there is no grain growth for the case that the peak temperature is 900°C because it is too small to cause grain growth. Also, the final sizes of prior austenite grain are determined as 30~38μm by using the temperature analysis results.

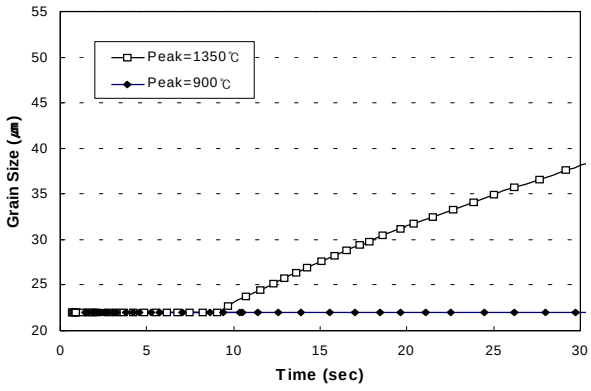

Fig. 6. Prior austenite grain growth according to peak temperature.

Prediction of CCT Diagram

To predict the CCT diagram of SA508 Gr.3 Cl.1, TTT diagram is determined by using the grain growth results and Li's reaction kinetics model(Ref. 11). And then the CCT diagram is

determined by using the TTT diagram and Scheil-Avrami addivity rule(Ref. 12, 13). Fig. 7 shows the predicted CCC diagram of SA508 Gr.3 Cl.1.

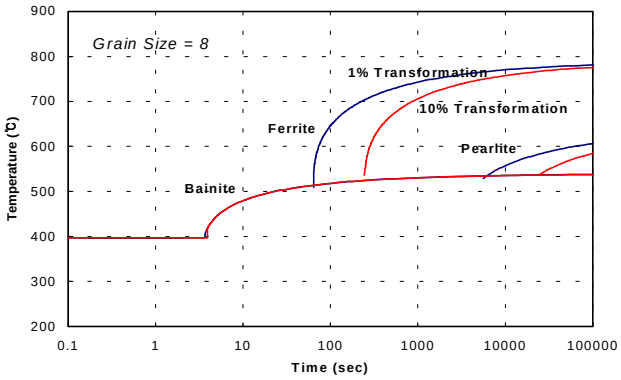

Fig. 7. Predicted CCT diagram of SA508 Gr.3 Cl.1.

Prediction of Precipitation Phases

By superposing the cooling curves obtained from temperature analysis on the predicted CCT diagram, the precipitation phases are determined according to cooling rate or distance from fusion line. As shown in Fig. 8, we can expect that only bainite and martensite will be formed over HAZ and the volume fraction of martensite will decrease with the increase of distance from fusion line.

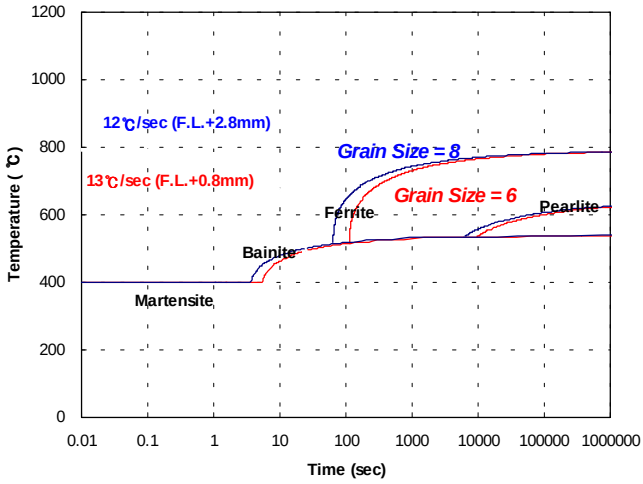

Fig. 8. Prediction of precipitation phases for SA508 Gr.3 Cl.1.

Estimation of Carbide Coarsening due to PWHT

Carbide coarsening during PWHT, which causes bainite microstructure to degrade hardness and ductility, is estimated by DICTRA(Ref. 14). Fig. 9 shows the estimation results of Mo_2C coarsening during PWHT. As shown in Fig. 9, we can expect that the carbide size will increase

by 30% as compared with initial size.

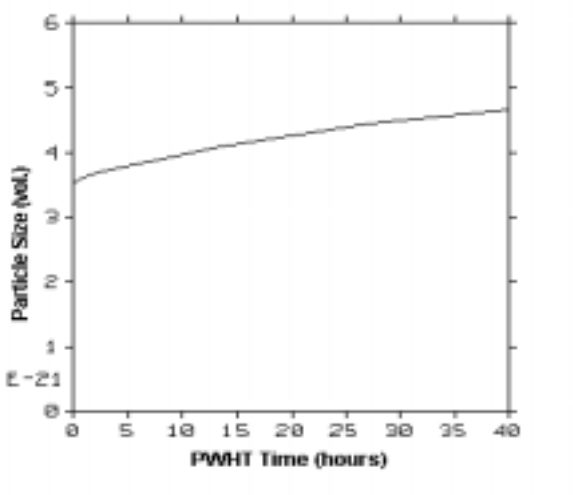

Fig. 9. Carbide coarsening due to PWHT.

5. MATERIAL PROPERTIES PREDICTION

Prediction of Hardness

The hardness of HAZ before PHWT is predicted by using the volume fractions of precipitation phases and the empirically based formulas(Ref. 15). Fig. 10 shows that the hardness decreases with the increase of distance from fusion line. Also, comparing with the experimental results(Ref. 16), the difference from the ones increases with the increase of distance from fusion line.

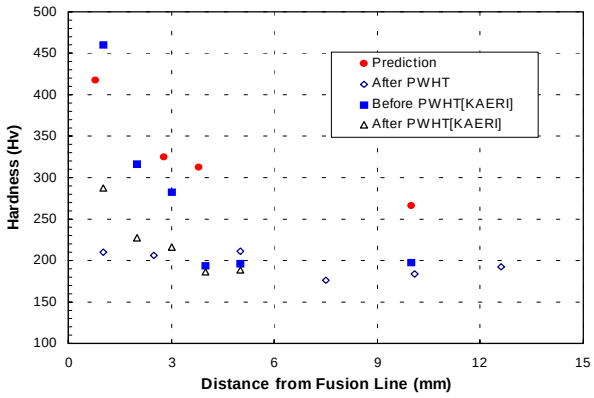

Fig. 10. Vickers hardness distribution according to distance from fusion line.

Estimation of Mechanical Strength

Yielding and tensile strength are estimated by the following relations(Ref. 17) between Vickers hardness and mechanical strengths:

$$\sigma_y = 3.1H_v(0.1)^n - 80 \quad (4)$$

$$o_u = 3.5H_v(1-n)\{12.4/(1-n)\}^n - 92 \quad (5)$$

$$n = 0.065(\Delta t_{800/500})^{0.17} \quad (6)$$

From Table 4, we can expect that the predicted results will be greater than the experimental results.

Table 4. Comparison between the predicted and the experimental mechanical strengths.

Location	H_v	$\Delta t_{800/500}$	Prediction (MPa)		Experiment (Ref. 18)
			σ_y	σ_u	σ_u
FL+0.8mm	417.6	23 sec	923.1	1648.2	1286
FL+2.8mm	325	25 sec	697.8	1265.8	1039

6. SUMMARY

In this study, the microstructures and material properties for HAZ of SA508 Gr.3 Cl.1 for the HAZ of RPV steel is estimated by using the temperature analysis, the thermodynamics-kinetics models and the empirical relations. The prediction results by applying this model show the reasonable agreement with the experimental results.

7. CONCLUSIONS

Based on the prediction results obtained from this study, the following conclusions can be made:

- Temperature cycle in HAZ is the saw-tooth pattern because of repeated heating and cooling during multi-pass welding.
- There is no grain growth for the case that peak temperature is 900^{o}C and the final sizes of prior austenite grain are also determined as 30~38μm.
- Only bainite and martensite are formed over HAZ and the volume fraction of martensite decreases with the increase of distance from fusion line.
- The carbide size increases by 30% during PWHT as compared with initial size.
- The as-welded hardness decreases with the increase of distance from fusion line.
- The predicted results for mechanical strengths are greater than the experimental results.

REFERENCES

1. Suzuki, K., et al., 2001, Nuclear Engineering and Design, 206, 261-278.
2. Kim, J.K. and Yoon, E.P., 1998, Journal of Nuclear Materials, 257, 303-308.
3. Alberry, P.J. and Lambert, J.A., 1982, The Welding Metallurgy of SA508 Cl.II Heat Affected Zones, Central Electricity Generating Board, TPRD/M/1223/R82.
4. Kussmaul, K., et al., 1982, Int. Conference on Welding Technology for Energy Applications, Gatlinburg, Tennessee, May 16-19, 17-69.
5. HKS Inc., 1998, ABAQUS User's Manual, Version 5.8.
6. Dong, P. and Brust, F.W., 2000, J. of Pressure Vessel Technology, 122, 329-338.
7. Thermo-Calc AB, 1999, Thermo-Calc User's Manual, Version M.
8. Atkins, M., 1980, Atlas of CCT Diagrams for Engineering Steels, ASM.
9. Hanjung Heavy Industry, 1996, Determination of Material Properties for SA508 Cl.III.
10. Svensson, L.E., 1993, Control of Microstructures & Properties in Steel Arc Welds, CRC Press.
11. Li, M.V., et al., 1998, Metallurgical and Materials Transactions B, 29B, 661-672.
12. Scheil, E., 1935, Arch. Eisenhuttenwes, 8, 565.
13. Avrami, M., 1939, J. Chem. Phys., 7, 1103.
14. Thermo-Calc AB, 1998, DICTRA User's Manual, Version 2.0.
15. Maynier, P., et al., 1978, Hardenability Concepts with Applications to Steels, AIME, 163-176.
16. Kang, S.Y., et al., 1999, J. of Korean Institute of Metals & Materials, 37(4), 423-434.
17. Akselsen, O.M., et al., 1990, Material Science and Technology, 6, 383.
18. Kim, J.H. and Hong, J.H., 2001, The 2nd Meeting for Welding Integrity Evaluation, KOPEC.